New analysis of a 50 years tide gauge record at Cananéia (SP-Brazil) with the VAV tidal analysis program

B. Ducarme
Chercheur Qualifié FNRS, Observatoire Royal de Belgique, Av. Circulaire 3, B-1180, Bruxelles, Belgique.

A.P. Venedikov
Geophysical Institute & Central Laboratory on Geodesy, Acad. G. Bonchev Str., Block 3, Sofia 1113

A.R. de Mesquita, C.A. de Sampaio França
Instituto Oceanográfico da Universidade de São Paulo, SP, Brasil.

D. S. Costa, D. Blitzkow
Escola. Politécnica, Universidade de São Paulo, Caixa Postal 61548, 05413-001 São Paulo, SP, Brasil.

R. Vieira Diaz
Instituto de Astronomía y Geodesia (CSIC-UCM). Facultad de Matemáticas. Plaza de Ciencias, 3. 28040. Madrid, Spain.

S.R.C. de Freitas
CPGCG - Universidade Federal do Paraná, Caixa Postal 19001, 81531-990 Curitiba, PR, Brasil.

Abstract. A homogeneous high quality tide gauge hourly record covering the period 1954-2004 was obtained at Cananéia (SP-Brazil). A previous analysis of a 36 years data set has shown many interesting features, especially very long period signals. This re-analysis benefits from a 40% longer time series and the powerful program VAV for tidal data processing is used to determine the parameters of the tidal constituents derived from the tidal potential, including the long period tidal waves, and of the shallow water and radiation tides. Long period terms are determined from the tidal residues by a semi-automatic research algorithm. The variation of the mean sea level is estimated after subtraction of the ocean tides and estimation of the long period terms. The mean sea level rate of change is estimated to 0.5666 ± 0.0070 cm/year. Special attention is given to the determination of the ocean pole tide as well as the 11 years term directly related to the solar activity.

Keywords. Ocean tides, mean sea level, ocean pole tide, radiation tides, Solar activity

1 Introduction

The paper presents some of the results from the application of the tidal program VAV (Venedikov et al., 2001, 2003, 2005) on the ocean tide (OT) data from the Cananéia tide gauge (SP- Brazil) (φ = 25° 01.0' S, λ = 47° 55.5' W). This series of data covers 50 years in the time interval 26.02.1954 – 31.12.2004 and contains 444410 hourly ordinates. A previous analysis of a 36 years data set (Mesquita et al., 1995, 1996) has shown many interesting features, especially very long period signals. The re-analysis benefits from the longer time series and a powerful tidal analysis program.

Tide gauge, station and data characteristics can be found in (Mesquita et al., 1983, 1995).

The present paper is mainly focusing on the investigation of the mean sea level (MSL), including its secular variation, and the detection of various low frequency components.

2 The VAV tidal analysis program

VAV is originally designed for the processing of Earth tide (ET) data. Now, it has been supplied by specific options (Ducarme et al., 2006a), corresponding to the OT characteristics and problems (Godin, 1972; Munk and Cartwright, 1966).

VAV has various options for tidal data processing. The main one for the OT is the determination of the amplitudes and the phases of all 1200 tides in the development of Tamura (1987), including the long period (LP) tides. For large series of data it can also study the time variations of the tidal parameters, as shown by Figure 1 for the tidal wave M2.

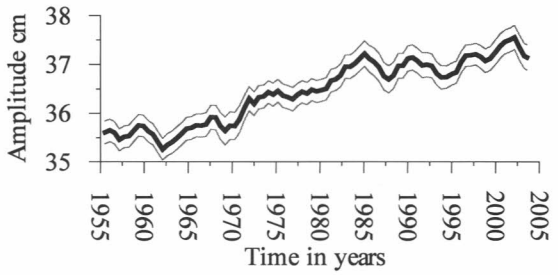

Fig. 1. Time variations of the amplitude of the main lunar tide M2 (thick line) with 95% confidence limits (grey lines) at Cananéia

The secular increase of the amplitude of M2 was already pointed out in Mesquita et al, 1995 and Harari et al, 2004. The amplitude seems more or less stable since 1985.

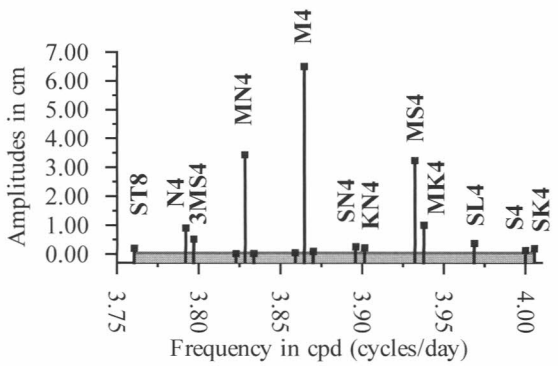

Fig. 2. Amplitudes of quarter-diurnal shallow water tides in Cananéia, the grey line representing the 99.99% confidence level.

VAV can also determine an arbitrary number of shallow water and radiation tides in the frequency bands from 1 till 12 cpd. The millimetre accuracy can be achieved (Figure 2).

Here we shall pay special attention to the investigation of the tidal residues $d(t)$ obtained by subtraction of the tidal signal. These residues should represent the sea level, free of the known tidal signals. However they can still include LP radiation tides with unknown periods. The investigation is made with the help of our computer program POLAR for regression and spectral analysis, initially created for the study of the gravity effect of the polar motion.

Figure 3 shows a sample of the sea level, determined by VAV. It is obtained after the reduction of all estimated tides, including the LP and the shallow water tides.

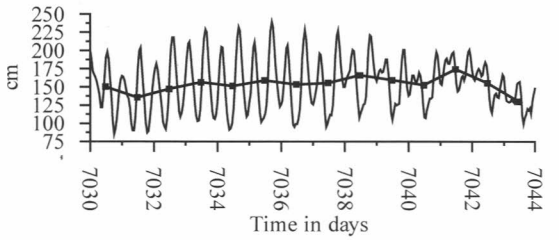

Fig. 3. Sample of the observed hourly tidal data and the residues (thick line), which represents the sea level, free of the tidal signals. The drift values $d(t)$ are determined every 24 hours (black dots).

Figure 4 represents the whole set of tidal residues or apparent sea level variations $d(t)$ (18570 daily values).

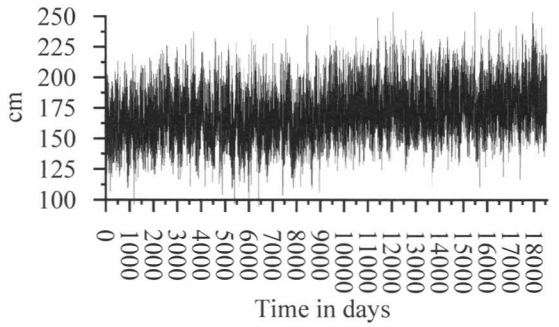

Fig. 4. The total curve of the sea level variations $d(t)$ (one value per day).

3 General model of the sea level variations

The general model used for $d(t)$ is

$$d(t) = L(t) + \sum_{j=1}^{M} W(\omega_j, t) \qquad (1)$$

The first term $L(t)$ is a polynomial of the time t, which we consider to represent the mean sea level (MSL).

Each term

$$W(\omega_j, t) = \alpha_j \cos \omega_j t + \beta_j \sin \omega_j t \qquad (2)$$

is a sinusoidal function of the time, representing a wave with frequency ω_j and unknown amplitude and phase. The frequencies, as well as their number M, are also a priori unknown quantities.

After many numerical experiments, combined with some theoretical considerations, we have accepted the hypothesis that the MSL $L(t)$ should be treated as a linear function, i.e.

$$L(t) = a_0 + a_1 t \tag{3}$$

with unknown regression coefficients a_0 and a_1. In such a way we accept that all non-linear components of $d(t)$ can be represented through the periodic terms $W(\omega_j,t)$, $1 \le j \le M$.

Once the model (3) is fixed, it remains to find the frequencies ω_j of the waves $W(\omega_j,t)$, i.e. we have to solve the problem of finding the hidden periodicities in the sea level $d(t)$.

4 Search of hidden periodicities

Our solution of the problem uses the Akaike Information Criterion AIC (Sakamoto et al., 1986), based on the principle of the maximum likelihood. The practical use of AIC is based on the following procedure. Let AIC(A) and AIC(B) be the values of AIC, obtained by the least square solutions using two different models A and B. If it happens AIC(A) < AIC(B), then we may give our preference to the model A.

At a given stage we know m frequencies, i.e. we have reached to the concrete expression of our model (1)

$$d(t) = L(t) + \sum_{j=1}^{m} W(\omega_j,t) \;\rightarrow\; \mathrm{AIC}(\omega_m) \tag{4}$$

Through the application of the least squares we get easily the estimates of all unknowns $a_0, a_1, \alpha_j, \beta_j$ $(1 \le j \le M)$, as well as the corresponding value of AIC, denoted $\mathrm{AIC}(\omega_m)$.

Next we add a new wave $W(\mathrm{w},t)$ with frequency w, which does not coincide with any of the existing frequencies ω_j, i.e. the expression (4) is replaced by

$$d(t) = L(t) + \sum_{j=1}^{m} W(\omega_j,t) + W(\mathrm{w},t) \;\rightarrow\; \mathrm{AIC(w)} \tag{5}$$

In the expression (5) the new frequency w is variable within a selected frequency interval. For every value of w we get the least squares solution of (5), accompanied by a corresponding value of AIC. In such a way we obtain AIC as a function of w, i.e. $\mathrm{AIC} = \mathrm{AIC(w)}$.

Let for a given value $\mathrm{w} = \mathrm{w_{Min}}$ $\mathrm{AIC(w_{Min})}$ be the minimum of the function $\mathrm{AIC(w)}$ in the frequency interval and, still, $\mathrm{AIC(w_{Min})}$ be lower than the previous AIC, i.e. $\mathrm{AIC(w_{Min})} < \mathrm{AIC}(\omega_m)$. This is accepted as a confirmation that one more wave $W(\omega_{m+1},t)$ with frequency $\omega_{m+1} = \mathrm{w_{Min}}$ really exist in $d(t)$, so that the expression (4) has to be replaced by

$$d(t) = L(t) + \sum_{j=1}^{m+1} W(\omega_j,t) \;\rightarrow\; \mathrm{AIC}(\omega_{m+1}) \tag{6}$$

The process is reiterated in the same way, by looking for a new frequency ω_{m+2}.

In the case of two close frequencies we can apply a 2D research algorithm for a minimum AIC. Instead of the model (5) with one new wave, we can add two waves with variable frequencies w' & w'', i.e. instead of (5) we use

$$d(t) = L(t) + \sum_{j=1}^{m} W(\omega_j,t) + W(\mathrm{w}',t) + W(\mathrm{w}'',t) \rightarrow \mathrm{AIC(w',w'')} \tag{7}$$

Now w' & w'' are allowed to cover two neighboring frequency intervals. For every couple w' & w'' we get the least square solution of (7), accompanied by a corresponding AIC value. In such a way we get $\mathrm{AIC} = \mathrm{AIC(w',w'')}$ as a function two frequencies. The values of w' & w'' at which AIC has a minimum can be accepted as two new frequencies ω_{m+1} and ω_{m+2}

As shown by Table 1 and Table 2 we have found in total $M = 16$ frequencies. We shall demonstrate the final stage of finding the first two of them, related with the Chandler period. Final stage means that we shall use first in (5), then in (7) $m = M - 2 = 14$ frequencies, namely those with numbers 3 to 16, while the two first frequencies will be found through frequency variations.

Figure 5 is obtained by the application of the model (5) where the variable frequency w is moving between 0.80 ÷ 0.95 cpy. Graphics like this one can be considered as an AIC spectrum.

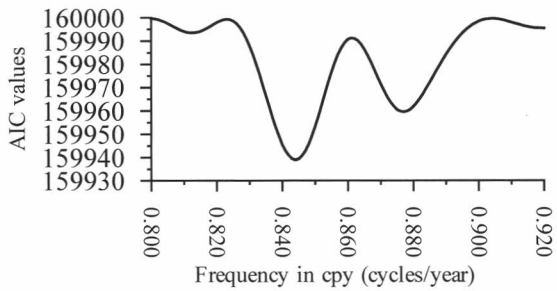

Fig.5. The values of $\mathrm{AIC} = \mathrm{AIC(w)}$ as function of the frequency w.

The absolute minimum of AIC in this case is at $w_{Min} = 0.84402$ cpy, i.e. at period 432.75 days. We have got also a relative minimum at frequency 0.87993 cpy, i.e. at period 415.09 days.

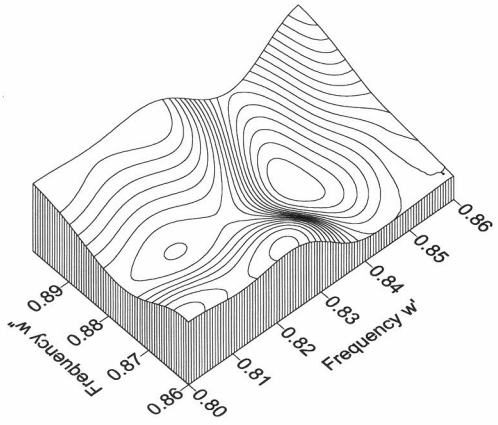

Fig. 6. $AIC = AIC(w', w'')$ with a minimum at $w' = 0.84180$ cpy and $w'' = 0.88102$ cpy.

Due to the existence of two minima at very close frequencies we had to apply the model (7). In such a way we get the picture presented by Figure 6, through which we get the final values of the first 2 components in Table 1.

The existence of two close periods at 433.6 and 414.3 day around the Chandler period of 430 day is due to the amplitude modulation of the signal.

Table 1. Summary of the periodicities found by the automatic research procedure for the Chandler term, the annual one and its harmonics

		Freq. cpy	Period Days	Amplit. cm	MSD cm
Chandler	1	0.8418	433.6	1.522	±0.188
	2	0.8810	414.3	1.271	±0.188
Annual 1 cpy	3	0.9973	366.0	5.111	±0.191
	4	1.0295	354.5	1.384	±0.192
Annual at 2 cpy	5	1.9881	183.6	1.241	±0.193
	6	2.0154	181.1	0.497	±0.193
Annual at 3 cpy	7	2.9189	125.0	0.945	±0.189
	8	2.9555	123.5	0.637	±0.189
	9	3.0298	120.5	0.912	±0.189

The usual spectral analysis deals with the amplitude spectrum, i.e. the amplitude, represented as a function of the frequency, looking for its maximum. Here we deal with AIC as a function of the frequency, looking for the minimum of AIC. A deeper difference is that the usual spectral analysis does not take in consideration the dependence between the frequencies found, which can be important when some of them are very close. On the contrary, our spectral analysis takes into account the effect of the frequencies already found, in this case of the $m = M - 2 = 14$ frequencies. The procedure can be repeated as many times as necessary in order to clean up completely such kind of dependences.

Table 2. Summary results for very low frequency components.

	Freq. cpy	Period Years	Amplit. cm	MSD Cm
10	0.0413	24.22	3.39	±0.21
11	0.0931	10.74	1.48	±0.19
12	0.1479	6.76	0.97	±0.19
13	0.1951	5.13	0.87	±0.19
14	0.2601	3.84	1.39	±0.19
15	0.3159	3.17	1.61	±0.19
16	0.3795	2.64	1.36	±0.19

As shown in Table 2 we have identified 7 very long periods. The component with the second largest period (10.74 years) corresponds to the known solar cycle with a period close to 11 years. Harmonics of this term are also present: 5.13 year (order 2), 3.84 and 3.17 (order 3) and 2.64 (order 4). The periodicity of 6.76 year, already found by Mesquita et al. (1995), is not easy to interpret, but could be the fourth harmonic of the longest period.

The total contribution to the sea level variations at Cananéia of periodicities longer than two year is plotted in Figure 7. The peak to peak amplitude (double amplitude) reaches 15 cm.

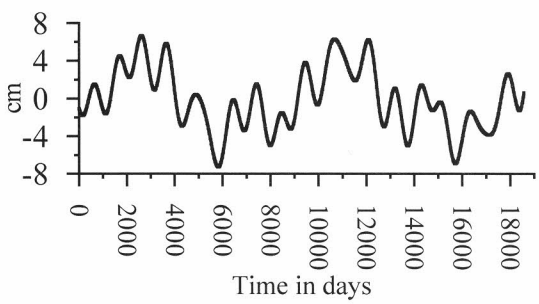

Fig. 7. Total contribution to sea level variations of the modeled periodicities with period larger than two years.

5 Evolution of the mean sea level

If M denotes the total number of the frequencies, the MSL $L(t)$, as it was defined by (3), is found through the least square solution of the model

$$d(t) = a_0 + a_1 t + \sum_{j=1}^{M} W(\omega_j, t) \qquad (8)$$

The use of the linear function $a_0 + a_1 t$ as representing $L(t)$ requires some explanations.

It appeared that when $L(t)$ is represented by a polynomial of power higher than 1, this polynomial interferes with the low frequency components, especially with the 24.2 year wave. Namely, we start getting too high coefficients of the polynomial with too high amplitudes of the periodic constituents. Due to this, we have accepted that the non-linearity in the development of $d(t)$ is entirely represented by the periodic constituents, while a reasonable representation of the MSL is by a polynomial $L(t)$ of power 1.

A problem in this simple model of $L(t)$ is whether there are not some discontinuities. Namely, whether there are not one or several time points T_{Disc} in which is an offset in $L(t)$, i.e. some changes in the constant a_0 or changes in the general behavior, i.e. changes in the coefficient a_1.

Testing the data in this sense is generally necessary for Earth tides data, since the gravimeters and the clinometers are suffering from offsets due to instrumental problems. It is rather unlikely to happen with tide gauges data, except during long interruptions of the records or inside interpolated sections.

Our conception is that in any case we should suppose possible discontinuities and check the data for their existence.

Let us check whether in a point T is a discontinuity. Then (8) should be used with different models of $L(t)$ before and after the point T, namely

$$\left.\begin{aligned} L(t) &= a_0' + a_1' t \quad \text{for } t \le T \\ L(t) &= a_0'' + a_1'' t \quad \text{for } t > T \end{aligned}\right\} \rightarrow \text{AIC}(T) \qquad (9)$$

We can let vary the point T in a time interval. For every value of T we can apply the least squares and thus obtain the AIC = AIC(T) as a function of T. If AIC(T) at $T = T_{\text{Min}}$ has a minimum and AIC(T_{Min}) is lower than AIC for the model (8), then we have to accept that T_{Min} is a point of discontinuity, i.e. $T_{\text{Disc}} = T_{\text{Min}}$.

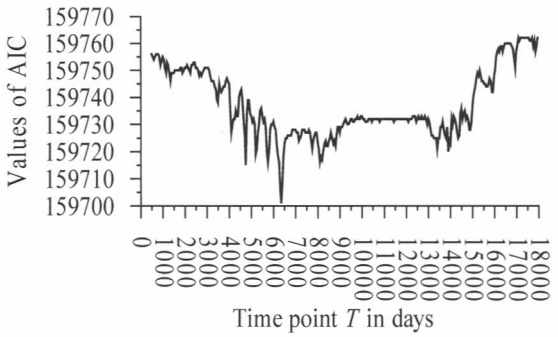

Fig. 8. AIC as a function of a supposed point T of discontinuity with T_{Min} = 6349 days (16.07.1971).

This is the case of Figure 8, showing a T_{Disc} = 6349 days. The result from the analysis with this T_{Disc} is shown in Figure 9.

A significant offset (jump) of 4.00 cm ± 0.68 cm has been found. However, the difference between the slopes of $L(t)$ before and after the discontinuity appeared to be not significant: 0.511 ±0.006 cm/year against 0.574±0.018 cm/year.

Other points of discontinuities have not been found.

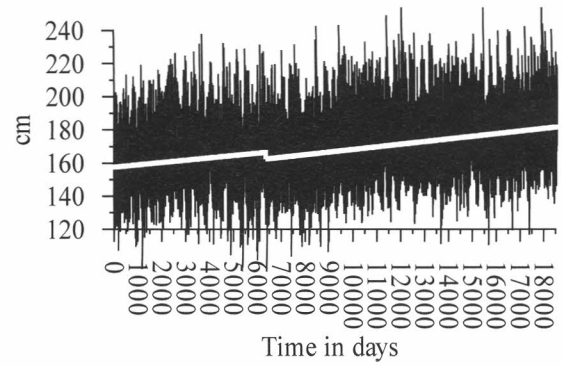

Fig. 9. The data $d(t)$ and the MSL $L(t)$ (white line) with a discontinuity in T_{Disc} = 6349 days.

On the basis of this result the data $d(t)$ have been corrected for the offset but, due to the lack of significant differences of the slopes before and after the jump, we applied later on the model (8) without discontinuity.

The final result about $L(t)$ are:

a_0 = 171.279 ± 0.094 at the epoch 31.01.1979
a_1 = 0.5666 ± 0.0070 cm/year

The slope is slightly higher than the 0.405 cm/year reported by Mesquita et al, 1995 or Harari et al, 2004.

6 Modeling of the ocean pole tide

The existence of Chandler frequencies indicates that the astro-geophysical phenomenon known as "ocean pole tide", generated by the polar motion, is effectively present in our data. The polar motion changes the position of the axis of rotation inside the Earth. At a given location on the Earth it produces a change of latitude measured by astronomical methods and a change of gravity, associated with the corresponding change of centrifugal force, measured by the superconducting gravimeters (Ducarme & al., 2006b). Moreover the associated P_2^1 potential is able to excite a tidal deformation of the sea surface.

In section 4 the study of the ocean pole tide was made in the frequency domain. It is certainly interesting to study the direct effect of the polar motion in the time domain.

At a point of coordinates (φ,λ) of the ocean surface, the equilibrium ocean pole tide can be written

$$p(t) = \gamma_2 \Omega^2 r^2 / 2g \cdot \{x(t)\cos\lambda + y(t)\sin\lambda\}\sin 2\varphi \qquad (10)$$

where $\gamma_2 = 1 + k_2 - h_2$, h_2 and k_2 being the Love numbers for radial deformation and change of the potential respectively, $x(t)$ and $y(t)$ are the coordinates of the pole at time t, Ω is the angular velocity of the Earth, r is the radius of the Earth and g is the acceleration of gravity.

The equilibrium pole tide has been computed for the daily coordinates of the pole, available from IERS since January 1, 1962, i.e. nearly 3000 days later than the start of the Cananéia data.

In analogy with the gravity effect of the polar motion (Ducarme & al., 2006b) we have accepted that the effect of the polar motion on our data $\Delta d(t)$ will be

$$\Delta d(t) = \delta_p p(t - \Delta t) \qquad (11)$$

where δ_p is an unknown regression coefficient, called also amplitude factor, and Δt is a time lag, positive for retardation.

This expression is included in our model in the following way

$$d(t) = a_0 + a_1 t + \sum_{j=1}^{M-2} W(\omega_j, t) + \delta_p p(t - \Delta t) \qquad (12)$$

Here we use only $M-2$ of the frequencies, the Chandler frequencies in Table 1 being excluded.

As we know already all $M-2$ frequencies, the only problem to estimate δ_p is the unknown Δt, which participates non-linearly in this model.

The problem has been solved by applying again a Bayesian approach, i.e. through the least square solution of (12) for a set of different values of Δt. In this case, since we are mostly interested in the values of δ_p we have chosen as a criterion the estimated MSD of this unknown. As shown by Figure 10 we get this MSD as a function of Δt. A broad minimum exists between 8 and 24 days, but we can accept, as a most reliable value of the time lag, the value of Δt at which we get the minimum of MSD i.e. $\Delta t = 21$ days. It means that the effect of the polar motion has 24 degrees of phase lag.

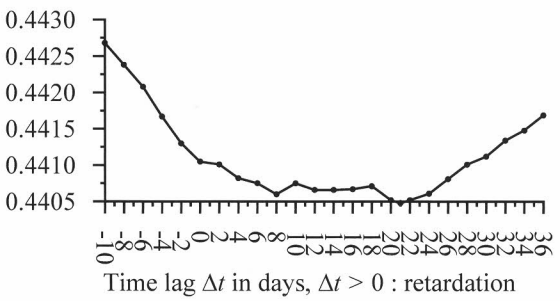

Fig. 10. MSD of δ_p as a function of the time lag Δt in the model (12), with a minimum at $\Delta t = 21$ days

Finally, by applying $\Delta t = 21$, we have got through the solution of (12) for the ocean pole tide an amplification factor $\delta_p = 2.19 \pm 0.44$.

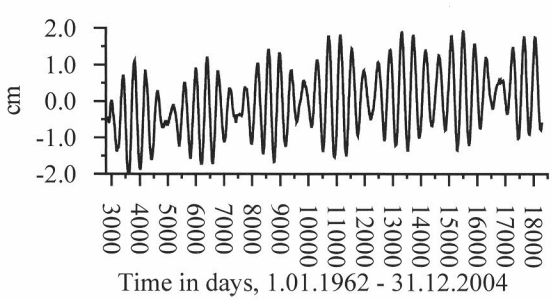

Fig. 11. Estimated ocean pole tide.

Figure 11 displays the estimated ocean pole tide at Cananéia, showing the effect of the secular drift of the pole position..

Using the model (12) the MSL variation becomes $a_1 = 0.547 \pm 0.014$ cm/year, with a lower precision than in the previous section. One of the reasons is that here a shorter series of data is used.

7 Modeling of the direct effect of the solar activity

Figure 12 shows the daily series of the sunspot index, measured by the number of Wolf $W(t)$, taken from the SIDC (Solar Index Data Center) (Vanderlinden et al, 2005). The series nearly coincides with the Cananéia ocean data. The phenomenon has obviously a period, very close to the period of our component 11 in Table 2.

Following the same idea as in the previous section we have attempted to study the direct effect of $W(t)$ on our data. The model now used is

$$d(t) = a_0 + a_1 t + \sum_{j=1}^{M-1} W(\omega_j, t) + \delta_W W(t - \Delta t) \quad (13)$$

where δ_W is an amplifying coefficient, Δt is a time lag, positive for retardation and $W(t)$ represents the solar activity. The number of waves is reduced by 1, because the component 11 is excluded.

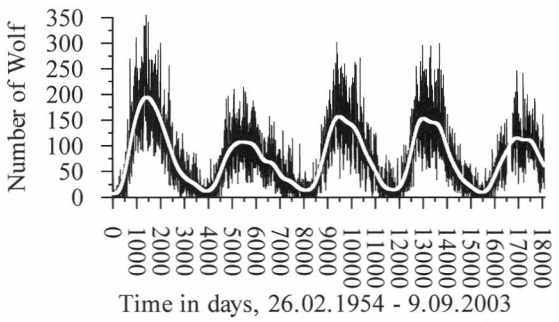

Fig. 12. Solar activity (sunspot index,, measured by the number of Wolf) and a least squares filtered variant (white curve): cut off 0.001cpd, half length 1,000 days.

We have used $W(t)$ in the following variants: (i) the raw data, (ii) filtered data by a least square low pass filtering with characteristics cut off frequency 0.003cpd, half length 300 and (iii) filtered with cut off frequency 0.001cpd, half length 1000 (the white curve in Figure 12).

In all cases, using the scheme illustrated in (Figure 10), we have got a zero time lag, i.e. $\Delta t = 0$.

With $\Delta t = 0$ in (13) we have got an estimate of δ_W with highest signal-to-noise ratio by using the smoothed data in variant (iii), namely $\delta_W = -1.88 \pm 0.28$ cm/(100 units of $W(t)$). It is thus in opposition of phase with the excitation.

The computed effect of the solar activity on the data is shown by Figure 13. It reaches a peak to peak amplitude of 4cm.

The estimated slope of $L(t)$ obtained in this way is $a_1 = 0.574 \pm 0.010$. Here again, as in the case of the polar data, the new value of a_1 does not differ significantly from a_1 in section 5 and, in the same time, it has a lower precision.

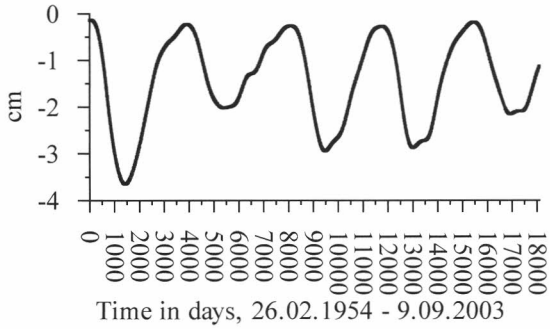

Fig. 13. Estimated effect of the solar activity on the ocean data.

8 Conclusions

An automatic procedure is used to determine hidden long period frequencies from the daily residues also called non-tidal components. The amplitude modulation of the annual radiation tide and its harmonic can be represented by a frequency splitting. The situation is similar for the Chandler period, associated with the ocean pole tide. Two periodicities dominate the very low frequency spectrum at 24.2 year and 10.7 year. The second one is clearly associated with the Solar cycle.

The ocean pole tide was modeled using the equilibrium tide. The results show an amplification factor close to 2 with a time lag between 10 and 24 days. In a similar way we tried to associate the 10.7 year period with the daily sunspot number. We found a perfect anti-correlation, without any time lag.

For what concerns the MSL variations, obtained after subtraction of the ocean tide signal and all the long period harmonic terms (pole tide and radiation tides), we found a mean linear drift rate of 0.5666 ± 0.0070 cm/year. This high rate is probably due to ground subsidence. GPS observations at the same site seem to confirm this fact (Blitzkow and Costa, personal communication). The necessity of a careful determination of the very long period harmonics for the estimation of MSL has to be underlined.

Acknowledgements

The work of A.P. Venedikov on this paper has been supported by the Royal Observatory of Belgium and the International Center for Earth Tides in Brussels and by the project REN2001-2271/RIES of the Institute of Astronomy and Geodesy in Madrid.

References

Ducarme B., Venedikov A.P., Arnoso J., Vieira (2005a). Analysis and prediction of ocean tides by the computer program VAV. *Journal of Geodynamics*, 41, 119-227.

Ducarme, B., Venedikov, A.P., Arnoso, J., , Chen X.D., Sun H.P., Vieira, R. (2005b). Global analysis of the GGP superconducting gravimeters network for the estimation of the pole tide gravimetric amplitude factor. *Journal of Geodynamics*, 41, 344-344.

Godin G., 1972. The analysis of tides. *Liverpool University Press,* 263 pp.

Harari J., França C. A. S., Camargo R. (2004). Variabilidade de longo termo de componentes de marés e do nivel medio do mar na costa brasileira.*http://www.mares.io.usp.br/aagn/aagn 8/ressi/ressimgf.html.*

Mesquita A.R., Harari J. (1983). Tides and tide gauges of Cananéia and Ubatuba-Brazil. *Relat. Int. Inst. Oceanogr. Univ. Sao Paulo*, 11, 1-14

Mesquita A.R., Harari J., França C.A. S. (1995). Interannual variability of tides and sea level at Cananéia, Brazil, from 1955 to 1990. *Publçao. Esp. Inst. Oceanogr., Sao Paulo,*11-20.

Mesquita A.R., Harari J., França C.A. S. (1996). Changes in the South Atlantic: Decadal and Interdecadal Scales. *An. Acad. Bras. Ci, 88 (Sup P1), 105-115.*

Munk, W. H., Cartwright, D. F. (1966). Tidal spectroscopy and prediction. Philosophical Transactions of the Royal Society of London A259 (1105) 533-581

Sakamoto, Y., Ishiguro, M., Kitagawa, G. (1986). Akaike information criterion statistics, *D. Reidel Publishing Company, Tokyo,* 290 pp.

Tamura, Y., 1987. A harmonic development of the tide-generating potential. *Bulletin Informations des Marées Terrestres*, 99, 6813-6855.

Vanderlinden R.A.M. and SIDC team (2005). On line catalogue of the sunspot index, http://sidc.oma.be/html/sunspot.html

Venedikov, A.P., Arnoso, J., Vieira, R. (2001). Program VAV/2000 for tidal analysis of unevenly spaced data with irregular drift and colored noise. *Journal of the Geodetic Society of Japan,* 47 (1), 281-286.

Venedikov, A.P., Arnoso, J., Vieira, R. (2003). VAV: a program for tidal data processing. *Computers & Geosciences*, 29, 487-502.

Venedikov, A.P., Arnoso, J., Vieira, R. (2005). New version of the program VAV for tidal data processing. *Computers & Geosciences*, 31, 667-669